I&EC research
Industrial & Engineering Chemistry Research

Article

pubs.acs.org/IECR

Formation of Copper−Neodymium Intermetallic Compounds by Carbothermic Reduction of Neodymium Oxide in the Presence of Copper

Ivar A. Ødegård* and Gabriella M. Tranell

Department of Materials Science and Engineering, Norwegian University of Science and Technology, NTNU, N-7491, Trondheim, Norway

Supporting Information

ABSTRACT: Carbothermic reduction of neodymium(III) oxide (Nd_2O_3) was performed by arc melting and in a graphite resistance furnace, using copper as a solvent metal. Successful carbothermic reduction was evident by formation of copper−neodymium intermetallics, where predominant phases were found to be Cu_6Nd and Cu_5Nd. The reduction reaction is proposed to be caused by thermal decomposition of neodymium oxide carbide ($Nd_2O_2C_2$) forming a molten mixture of neodymium(III) oxide and neodymium dicarbide (NdC_2) upon release of carbon monoxide (CO(g)), where subsequent decomposition of neodymium dicarbide was facilitated by a reduction in activity of formed elemental neodymium species solvated in molten copper. Addition of carbon in excess of neodymium oxide carbide stoichiometry was found to correlate with increased concentration of neodymium in copper, likely caused by an increase in concentration of neodymium dicarbide.

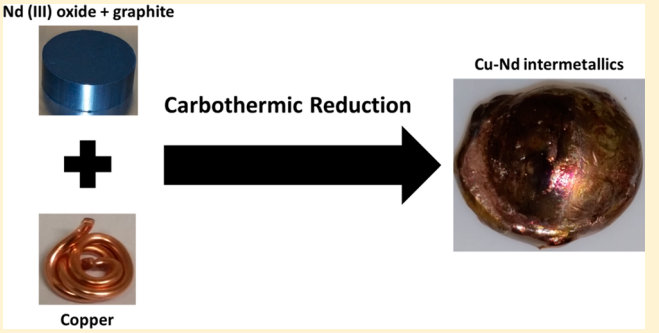

INTRODUCTION

Rare earth elements (REEs) are of increasing importance with the transition into a greener economy.[1] Neodymium (Nd) is recognized by multiple nations as a light rare earth element of critical importance, due to increasing use in applications ranging from catalysis to electronics and permanent magnets.[2−4] Synthesis of elemental Nd was originally performed by calciothermic reduction, where Nd(III) species (chloride, fluoride, oxide etc.) were reduced by elemental calcium, forming elemental Nd.[5] The calciothermic reduction route, being a batch process, made the process labor intensive and time-consuming, driving up its production cost. Modern production of elemental Nd utilizes molten salt electrolysis, allowing for continuous production of the element along with higher product purity. With this method, Nd species in the form of oxides, fluorides, or chlorides are fed to a molten bath consisting of chlorides or fluorides, being electrochemically reduced.[6] Molten salt methods are however not without drawbacks; molten chlorides have low current efficiency as well as being hygroscopic, operating below the melting point of elemental Nd, requiring formation of an alloy with a melting point below that of the chloride bath in order to avoid dendrite formation and vaporization of the electrolyte.[7] Molten fluoride electrolytes, on the other hand, have low solubility of neodymium(III) oxide (Nd_2O_3). This necessitates close control of feedstock addition in order to avoid sludge settling to the cell bottom, anode effect, and bath compositional changes as a function of feedstock content.[8] As such, more energy efficient, high productivity methods of producing and recycling Nd are sought.

Due to the high affinity between rare earth elements and carbon, forming a range of stable carbides and oxide carbides, carbothermic reduction as a method of producing the corresponding elemental compounds has been considered to be difficult at best.[9] From available literature, several accounts of carbothermic reduction with respect to elements that are known to form stable carbides were found, among these, the rare earths are represented. Some methods mentioned are reduction by dissolving into suitable solvent metals, reaction between carbides, and an element forming a more stable carbide, formation of nitrides then vacuum decomposition of said nitrides in solution with suitable solvent metals, etc.[10−18] Examples from literature reveals, among others, a patent by Staggers that describes carbothermic reduction of rare earth elements by formation of rare earth silicide alloys.[18] The method apparently allows for the simultaneous carbothermic reduction of rare earth oxides, especially cerium oxide (CeO_2) along with alkaline earth oxides such as barium oxide (BaO), calcium oxide (CaO), and strontium oxide (SrO) in the presence of silica (SiO_2) and elemental iron (Fe) at elevated temperatures, forming both rare earth and alkaline earth

Received: July 9, 2018
Revised: August 30, 2018
Accepted: September 13, 2018
Published: September 13, 2018

DOI: 10.1021/acs.iecr.8b03117
Ind. Eng. Chem. Res. XXXX, XXX, XXX−XXX

silicides.[18] A later patent by Gschneider et al. describes reduction of rare earth oxides by use of carbon as reductant. The patent discloses reduction of Nd and praseodymium (Pr) in the presence of elements like silicon (Si), germanium (Ge), tin (Sn), lead (Pb), arsenic (As), antimony (Sb), and bismuth (Bi). In addition to the reduction of the above-mentioned Nd and Pr, the possibility of performing carbothermic reduction of other rare earths like lanthanum (Ln), cerium (Ce), samarium (Sm), europium (Eu), gadolinium (Gd), terbium (Tb), dysprosium (Dy), holmium (Ho), and thulium (Tu) were mentioned.[14] It is interesting to note that the patents of both Staggers and Gschneider et al. mentioned formation of rare earth silicides, yet no mechanism of formation was given in either patent.

When addressing problems regarding formation of stable carbides during carbothermic reduction, a method proposed by Anderson and Parlee circumvents problems associated with formation of such carbides. With this method, dissolution of the reactive elemental compounds into a solvent metal (Sn) is performed, hence lowering chemical activity of an element below that required for carbide formation. The method allows for carbothermic reduction of oxides of Zr, Mg, Ti, Si, Al, and U, while direct carbothermic reduction of rare earth elements was not mentioned.[11,19] An example with respect to use of carbides was found in a patent by Mcallum et al. which describes carbothermic reduction of Nd_2O_3, forming neodymium sesquicarbide (Nd_2C_3) or neodymium dicarbide (NdC_2) that was subsequently reacted with $TiFe_2$ and Fe_2B, forming an Fe−B−Nd alloy. The assumed mechanism was that titanium would form a carbide of higher stability than any Nd-carbides. According to the patent, evidence of finely dispersed titanium carbide (TiC) was found to exist within the sample.[16] The general chemical reactions governing carbothermic reduction of oxides by metal solvent are (I−IV):

Carbothermic reduction of the oxide (I):

$$M_xO_y + yC \rightarrow xM + yCO(g)$$

Solvation of the solute metal(II):

$$xM_A \rightarrow xM_{A(solvated)}$$

Formation of an intermetallic (III):

$$xM_{A(solvated)} + zM_{B(Solvent)} \leftrightarrow M_{(A)x}M_{(B)z}$$

The major competing reaction concerns the formation of carbides (IV):

$$xM + nC \rightarrow M_xC_n$$

According to work performed by Anderson and Parlee as reviewed by Selvaduray, the significant factors regarding choice of solvent metal include formation of stable intermetallic compounds, along with melting and boiling point, density, abundance of solvent metal, solubility of other metals, reactivity toward gaseous species, and carbon solubility.[11,17] Intermetallic compounds should preferably display high melting points, indicative of high affinity between solvent and solute metal. Density determines if oxide material being subject to reduction either floats or sinks in the liquid solvent metal, influencing the surface area available for reaction to occur.[17] Boiling point was found to be important with respect to separation of formed product from solvent metal when vacuum distillation was employed as well as the ability to maintain a low pressure atmosphere during the reduction.[17] Carbon solubility is another important feature with respect to choice of solvent metal, meaning that the solvent metal should have negligible carbon solubility. Suitable solvent metals should also be abundant in nature and preferably nontoxic. Any solvent metal should also display limited reactivity with respect to gaseous species like nitrogen ($N_2(g)$) and oxygen ($O_2(g)$).[17] Partial pressure of carbon monoxide (CO(g)) must be kept below equilibrium, shifting the reaction to the product side, according to Le Chatelier's principle. Removal of CO(g) is usually achieved by continuous vacuum pumping or continuous flushing with inert gas.[10,11] According to available literature, depending on type of oxide to be reduced, metals displaying desired properties with regards to acting as solvent metals are tin (Sn), copper (Cu), lead (Pb), bismuth (Bi), antimony (Sb), iron (Fe), and silicon (Si).[10,11,20,21] The feasibility of carbothermic reduction with respect to an oxide in a solvent metal depends on the activity of the solute metal in a solvated or intermetallic state. The activity must be below values required for the formation of corresponding carbides. Should the solute metal activity be kept lower than mandated by the equilibrium constant representative of the carbide formation, decomposition of the carbide into carbon and metal constituents would be expected, provided kinetic barriers are absent.[17] It is well-known that copper has a very low carbon solubility and forms several intermetallics with neodymium (Nd). It also features a high boiling point which make it a suitable solvent metal for investigating carbothermic reduction of neodymium oxide.[22−25] Carbothermic reduction of Nd_2O_3 in absence of a metal solvent will form either the oxide carbide ($Nd_2O_2C_2$) or the dicarbide (NdC_2) depending on the available quantity of carbon, partial pressure of carbon monoxide (CO(g)) and the temperature.[26,27] Information on the Nd−O−C system is unfortunately scarce, and only one paper by Butherus et al. was found on the synthesis and properties of $Nd_2O_2C_2$.[26] The current work thus, initially, addresses carbothermic reduction of Nd_2O_3 in the presence of graphite, to evaluate thermal behavior of the $Nd_2O_2C_2$ phase. Subsequently, reactants featuring final $Nd_2O_2C_2$ stoichiometry were reduced by utilizing copper as a solvent metal and then analyzed to determine final product composition.

EXPERIMENTAL SECTION

In the following section, much care has been taken to elaborate on the experimental aspects of this work, since sample preparation, handling, and analysis were challenging due to the extreme reactivity of the materials.

Materials. Reactant samples were produced from neodymium(III) oxide (Nd_2O_3, 99.9% REO, Alfa Aesar) and graphite (TC 307, 99.9%, Cummings-Moore Graphite). Before any mixing of reactants took place, Nd_2O_3 was annealed in a muffle furnace (1000 °C, 2 h, Nabertherm N17/HR) to remove carbon dioxide ($CO_2(g)$) or water (H_2O) that easily reacts with the compound. After annealing, Nd_2O_3 was transferred to a desiccator featuring strong desiccants (molecular sieves, 3 Å, Alfa Aesar and phosphorus pentoxide, P_2O_5, 98%, Alfa Aesar) and allowed to cool. Heat treatment was also performed for graphite by annealing in an outgassed graphite tube furnace featuring inert gas (1700 °C, 2 h, Ar, 99.9999%, AGA) and graphite crucibles. For the remainder of this paper any use of the term "inert gas" refers to gas of the previously mentioned type, quality, and manufacture. Heat treatment of the graphite was done to remove volatiles and adsorbed species that could interfere with measurements and

DOI: 10.1021/acs.iecr.8b03117
Ind. Eng. Chem. Res. XXXX, XXX, XXX−XXX

experimental conditions. Reactants were weighed out on an analytical scale (Mettler-Toledo XPE 504DR) before mixing (20 min, WAB Turbula Mixer T2C) and ring milling (3 × 2 min, Herzog HSM 100H, tungsten carbide milling rings). After milling, reactant samples were pressed into cylindrical pills (10 mm diameter, 2.0-ton, 1.0 min, Compac DP10-B). Reactant pills were subsequently annealed in a graphite resistance furnace featuring continuous purging with inert gas (1300 °C, 2 h, 0.5 slpm). This was to avoid reactant pills breaking up during reaction, causing potential problems with respect to product composition. Post annealing, tablets were used directly in subsequent reduction experiments. Reactant stoichiometry was chosen to allow formation of the compound neodymium oxide carbide ($Nd_2O_2C_2$). This compound has previously been thoroughly investigated by Butherus et al.[26,28] The quantity of carbon was also varied in order to elucidate information on the reaction mechanism. Copper (Cu, 99.9%, Alfa Aesar) was acquired in the form of plates or wire, cleaned (*n*-heptane, 99%, Merck), dried, and cut to the necessary quantity.

CARBOTHERMIC REDUCTION PROCEDURES

Carbothermic reduction of Nd_2O_3 was carried out through two approaches: reaction within a tungsten crucible in a graphite resistance furnace and arc melting, respectively. A set of initial experiments were performed to investigate thermal behavior of the $Nd_2O_2C_2$ phase at elevated temperature (1600−1900 °C). These initial experiments featured exclusive use of a resistance heated graphite furnace and tungsten crucibles. Use of a graphite resistance heated furnace means that high temperatures are attainable at all but an oxidizing atmosphere. It also allowed for close control of both temperature and atmospheric conditions. Arc melting is fast and makes visual control of the process possible, permitting several experiments to be performed in short time and even if tight control of temperature could prove challenging, the atmosphere could be reasonably controlled. Arc melter experiments also provided a way to reduce tungsten contamination of the final products since spectroscopic grade graphite rod was utilized as an electrode material instead of the tungsten electrode usually employed by this instrument. Results acquired from arc melter experiments were thought to give an indication on possible future scalability of the process by utilizing pre-existing electric arc furnace technology. An outline of the experimental parameters followed during initial experiments is presented in Table S1 of the Supporting Information, whereas experimental parameters for the main work regarding carbothermic reduction of Nd_2O_3 in the presence of copper are presented in Table S2 of the Supporting Information. Two copper stoichiometries were chosen as to determine the maximum attainable Cu−Nd intermetallic, between the Cu_6Nd and Cu_2Nd stoichiometries. The carbon content was varied to elucidate the underlying reaction path and mechanism.

Method 1: Reduction in Graphite Resistance Furnace. Reduction in the graphite tube furnace was performed by filling a tungsten crucible with appropriate amounts of elemental copper and previously annealed reactant pills. The crucible was then quickly transferred to an outer graphite crucible and placed in the furnace which was subsequently repeatedly evacuated and purged with inert gas (3×) before being heated and maintained at elevated temperature (1900 °C, 4 h).

During annealing the furnace was continuously flushed with inert gas (0.5 slpm) to ensure continuous dilution and removal of formed CO(g). During preliminary experiments, the furnace was also flushed with CO(g) (0.5 slpm) to evaluate stability of products toward this gas at a certain temperature. A sectional view of the graphite tube furnace is presented in Figure 1.

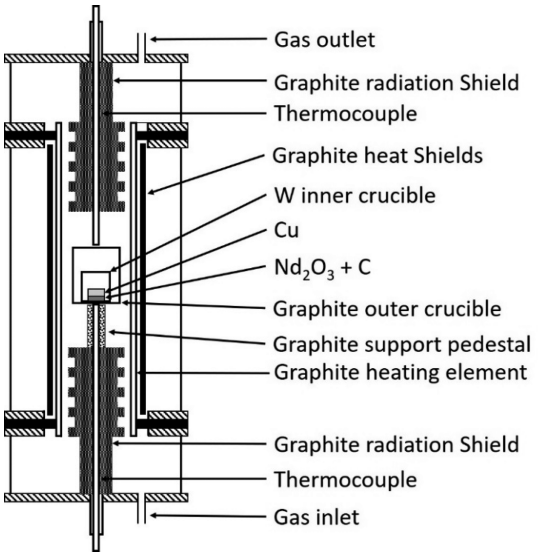

Figure 1. Graphite resistance furnace, schematical view of setup.

Upon cooling of the furnace, the crucible was removed and quickly filled with mineral oil (High Purity, Amresco) to reduce possible detrimental interactions with atmospheric species such as oxygen, carbon dioxide, and moisture. All samples were stored in glass desiccators.

Method 2: Arc Melting. Carbothermic reduction featuring arc melting involved placing annealed reactant pills in an arc furnace (Compact Arc Melter, MAM-1, Edmund Bühler GmbH) along with an appropriate amount of elemental copper (99.9%, Alfa Aesar). The furnace was repeatedly vacuumed and purged with high-purity inert gas, in addition, an oxygen getter (Zr, 99.95%, Alfa Aesar) was arc melted before any reactants to further reduce oxygen partial pressure. The initial tungsten (W) electrode was later replaced by a graphite electrode (spectroscopic grade, Ted Pella Inc.) to avoid W contamination of the sample materials. A sectional view of the arc melter is given in Figure 2.

Samples were then sequentially alternated between arc melting of an oxygen getter, arc melting of the reactants (5 × 1

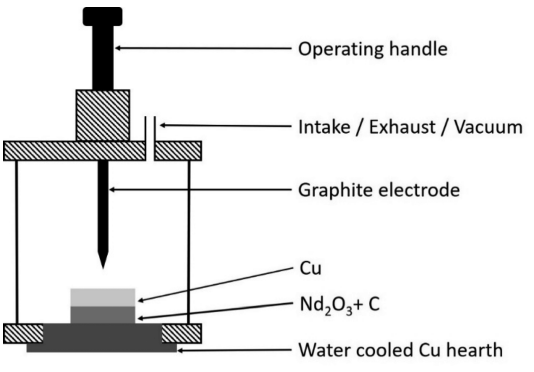

Figure 2. Arc melter, schematical view of experimental setup.

DOI: 10.1021/acs.iecr.8b03117
Ind. Eng. Chem. Res. XXXX, XXX, XXX−XXX

min), followed by vacuum pumping and purging of the furnace chamber with clean inert gas; this was done to ensure removal of CO(g). After arc melting, samples were quickly transferred to a sealed container featuring mineral oil (High Purity, Amresco). All sealed sample containers were then stored in glass desiccators.

SAMPLE ANALYSIS

Electron Micro Probe Analysis (EPMA). Analysis of samples reacted in the graphite resistance furnace involved milling chips from the metal sample by placing oil filled crucibles featuring metal samples in a universal milling machine (Knuth, VHF2, tungsten carbide tooling). Produced metal chips were quickly collected and cleaned (*n*-heptane, 99%, Merck) before being transferred to a hot press (Struers Labopress-1) and fixated using a hot mounting resin (Polyfast, 180 °C, 5 min residence time, 3 min cooldown time, 15 kN pressing force). Fixated samples were then polished using successively finer abrasives starting with silicon carbide discs going up to magnetic discs (MD-Largo, MD-Mol, MD-Nap, Struers Inc.) featuring diamond suspension (9, 6, and 1 μm, Struers Inc.). During sample preparation such as grinding and polishing, all grinding media and samples were continuously supplied fresh inert oil to keep oxidation to a minimum. Material stemming from arc melting was in the shape of beads and was not found to require fixation. These samples were therefore only subjected to an identical grinding and polishing step as for samples featuring fixated chips, forming coin like structures with highly polished surfaces. Immediately before EPMA analysis, polished samples were cleaned thoroughly with *n*-heptane to remove any adhering mineral oil and then quickly transferred to an EPMA analyzer (JEOL JXA-8500F, EPMA) where elemental distribution among various phases were identified and quantified. This was done to avoid detrimental oil contamination of instrument high vacuum chambers along with minimizing time for exposure of sample material to atmospheric species. In EPMA, phases enriched in heavier elements were brighter than phases featuring lighter elements. A visual indication of element concentration is provided by the accompanying color scale for each respective analyzed element where the darker end of the scale indicates low concentration and brighter end indicates higher concentration.

X-ray Diffraction Analysis (XRD). For X-ray diffraction analysis (XRD, Bruker D8 Focus, Cu Kα radiation (λ = 1.5418 Å)), chips from milling were transferred to an agate mortar and completely immersed in mineral oil before being carefully ground down, using an agate pestle, until it had the consistence of a fine slurry. Upon XRD analysis, slurry samples were transferred to a paper towel to remove as much mineral oil as possible before being carefully spread out on XRD sample holders. This method was also employed for the initial experiments on the $Nd_2O_2C_2$ phase. With respect to materials resulting from the arc melting process, samples that had been ground and polished to a coin like structure as described in sample preparation for EPMA analysis, were used directly in XRD analysis. These samples were fixated on the XRD sample holder by using silly putty between holder and sample to be analyzed. Mineral oil was applied to surfaces exposed to atmosphere to avoid oxidation of samples during analysis. Note that for the initial experiments, the 2θ axis starts from 10 deg, whereas for the main experiments it starts from 20 deg. This was done to increase legibility, since much information is presented in a relatively narrow 2θ range. No information on importance was lost this way as compared to original diffractograms.

RESULTS

Reactions of consideration with respect to carbothermic reduction of Nd_2O_3 to form a Cu−Nd intermetallic, as generally described in the Introduction are

1. Direct carbothermic reduction of Nd_2O_3 to elemental neodymium (hypothetical reaction due to high stability of corresponding oxide carbide/carbide):[29]

$$Nd_2O3(s) + 3C(s) \rightarrow 2Nd + 3CO(g)$$

$$\Delta G^{\circ}_{1900^{\circ}C} = 294.549\ \text{kJ}$$

2. Formation of $Nd_2O_2C_2$ (insufficient thermodynamic data at given temperature):[26,29]

$$Nd_2O_3(s) + 3C(s) \rightarrow Nd_2O_2C_2(s) + CO(g)$$

3. Thermal decomposition of $Nd_2O_2C_2$ (insufficient thermodynamic data at given temperature):[26,29]

$$\frac{7}{2}Nd_2O_2C_2(s) \rightarrow 2Nd_2O_3(s) + 3NdC_2(s) + CO(g)$$

4. Formation of neodymium carbide:[29]

$$Nd(l) + 2C(s) \rightarrow NdC_2(s)$$

$$\Delta G^{\circ}_{1900^{\circ}C} = -360.791\ \text{kJ}$$

5. Decomposition of neodymium dicarbide by solvation of Nd in a solvent metal (e.g., Cu):[29]

$$NdC_2(s) \rightarrow \underline{Nd}(l) + 2C(s)$$

$$\Delta G^{\circ}_{1900^{\circ}C} = 360.791\ \text{kJ}$$

6. Formation of neodymium copper intermetallics (thermodynamic expressions featuring Gibbs energy of formation for each of the intermetallic compounds are given in J/mol) (parts a−e, ref 30; part f, ref 23):

(a) $\underline{Nd}(l) + 6Cu(l) \rightarrow Cu_6Nd(s)$

$$\Delta G^{\circ}_{fCu_6Nd} = -25369 + 8.53T$$

(b) $Nd(l) + 5Cu(l) \rightarrow Cu5Nd(s)$

$$\Delta G^{o}_{fCu_5Nd} = -20749 + 3.29T$$

(c) $\underline{Nd}(l) + 4Cu(l) \rightarrow Cu_4Nd(s)$

$$\Delta G^{\circ}_{fCu_4Nd} = -18078 + 0.65T$$

(d) $\underline{Nd}(l) + 2Cu(l) \rightarrow Cu_2Nd(s)$

$$\Delta G^{\circ}_{fCu_2Nd} = -39059 + 14.07T$$

(e) $\underline{Nd}(l) + Cu(l) \rightarrow CuNd(s)$

DOI: 10.1021/acs.iecr.8b03117
Ind. Eng. Chem. Res. XXXX, XXX, XXX−XXX

$$\Delta G^{\circ}_{fCuNd} = -32086 + 9.64T$$

$$(f)\ 2\underline{Nd}(l) + 7Cu(l) \rightarrow Cu_7Nd_2(s)$$

$$\Delta G^{\circ}_{fCu_7Nd_2} = -10046.4 - 7.2194T$$

According to information on the phase diagram of Cu−Nd, Cu_6Nd has the highest melting point of the above listed compounds and the melting points of the Cu−Nd intermetallics are found to drop as the concentration of Nd increases.[30−32] The phase diagram as generated by use of Factsage software is presented in Figure 3.[33] This phase

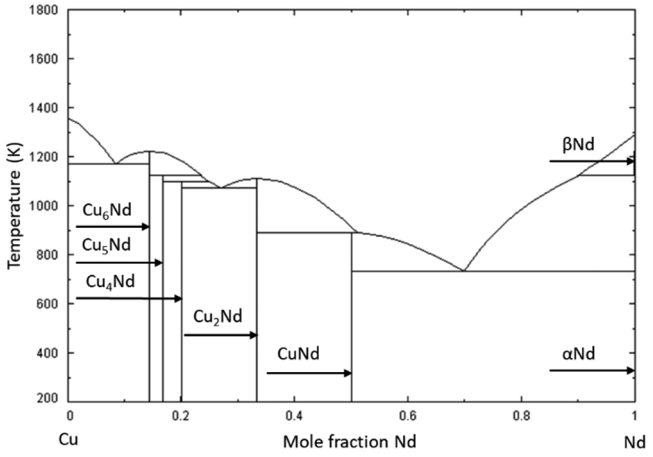

Figure 3. Phase diagram of Cu−Nd system.

diagram is found to correspond with a phase diagram suggested by Subramanian and Laughlin although no literature reference was given in the Factsage database.[30] It is however observed that this database has omitted the Cu_7Nd_2 phase, although reported by these authors as well as by Carnasciali et al.[25,30]

Initial Experimental Work on the $Nd_2O_2C_2$ Phase. As there is no reliable phase diagram for the Nd−O−C system available in the literature, a set of initial "system mapping" experiments to assess the melting behavior of Nd−C−O compounds, was carried out (1600−1900 °C, 2−7 h, experiments 1−4 in Table S1).

The mixture comprising Nd oxide carbide was found to be partially molten when subjected to a temperature of 1600 °C in a continuously flushed atmosphere of inert gas for 7 h. This is illustrated in Figure 4, where a stack of reactant pills were fused together. Since visual details of the initial pills and stackstill can be made out, it is assumed that the mixture has been only partially molten.

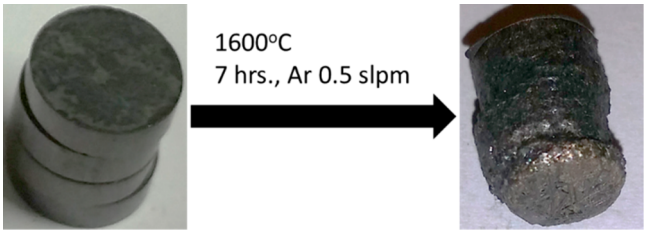

Figure 4. Initial experiment with reactants mixed to $Nd_2O_2C_2$ stoichiometry and subjected to heating at 1600 °C for 7 h.

Results of XRD analysis of the reactant mixture subjected to extended heating at 1600 °C is presented in Figure 5. The material is found to consist of mostly $Nd_2O_2C_2$ with traces of Nd_2O_3.

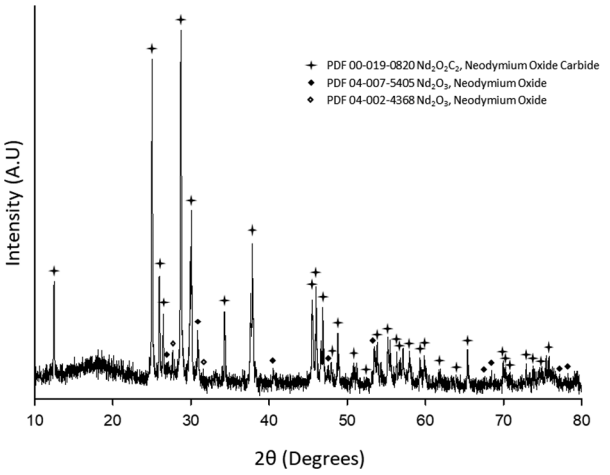

Figure 5. XRD analysis of reactants mixed to $Nd_2O_2C_2$ stoichiometry and heated at 1600 °C for 7 h.

Increasing temperature to 1900 °C resulted in the mixture becoming molten, forming a reflective compound with a brass or golden color as is presented in Figure 6. The material was

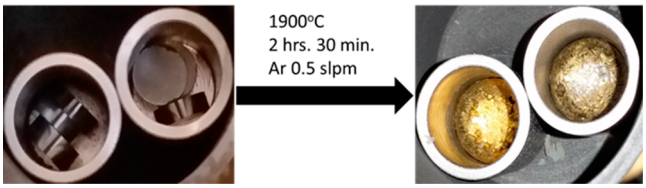

Figure 6. Initial experiment featuring reactants mixed to $Nd_2O_2C_2$ stoichiometry and heated in continuously flushed inert gas atmosphere.

found to be extremely sensitive to moisture and quickly tarnish in air, leaving an ash like powder with a blue tint, releasing extremely flammable acetylene as it was tarnishing.

The experiments also involved subjecting the reactants to different atmospheres (Ar, CO(g)) to assess potential effect on equilibrium products. Melting in an atmosphere of continuously flushed inert gas was also found to be accompanied by thermal decomposition of the $Nd_2O_2C_2$ compound. According to XRD analysis of a sample subjected to melting in inert gas, as presented in Figure 7, the sample was found to consist of a fused mixture of Nd_2O_3 and NdC_2 along with only traces of $Nd_2O_2C_2$.

The decomposition reaction was sensitive to partial pressure of carbon monoxide (CO(g), as expected from reaction 3), since experiments featuring use of CO(g) ($P_{CO(g)}$= 1 atm, T = 1900 °C, 2 h, 30 min) instead of inert gas did not display the same melting behavior as experiments featuring inert gas atmosphere. Instead the reactant pills were intact, only displaying small metallic gray droplets on the surface as can be seen in Figure 8.

Results from XRD analysis of a sample heated in a constantly flushed atmosphere of CO(g) is given in Figure 9. The sample was found to consist of Nd_2O_3 and graphite with

DOI: 10.1021/acs.iecr.8b03117
Ind. Eng. Chem. Res. XXXX, XXX, XXX−XXX

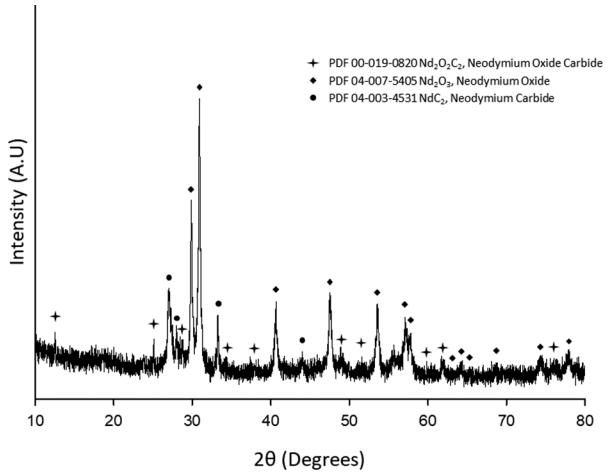

Figure 7. XRD analysis of thermally decomposed Nd oxide carbide at 1900 °C in continuously flushed inert gas atmosphere for 2.5 h.

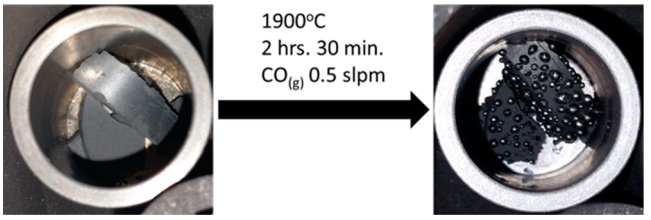

Figure 8. Initial experiment featuring reactants in $Nd_2O_2C_2$ stoichiometry heated in a continuous CO(g) atmosphere.

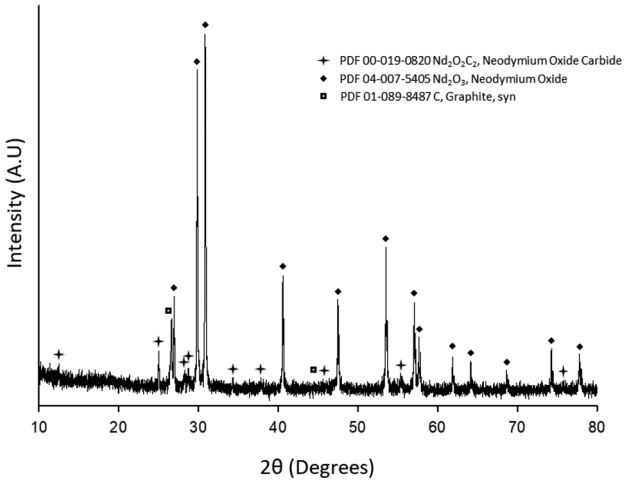

Figure 9. XRD analysis of a sample featuring $Nd_2O_2C_2$ stoichiometry subjected to heating at 1900 °C in continuously flushed CO(g) atmosphere for 2.5 h.

faint diffractions of $Nd_2O_2C_2$. To evaluate the stability of the apparently molten mixture of Nd_2O_3 and NdC_2 as discovered in the first experiment, toward CO(g), a new experiment was devised. In this experiment the reactants were heated and subjected to inert gas (1900 °C, 30 min, Ar) before changing atmosphere to CO(g) while maintaining identical temperature (1900 °C, 2 h).

f10 As illustrated in Figure 10, reactants had melted and formed a gray, reflective metallic looking material, much different from the brass looking material observed in the first experiment. This material was also found to be extremely reactive toward

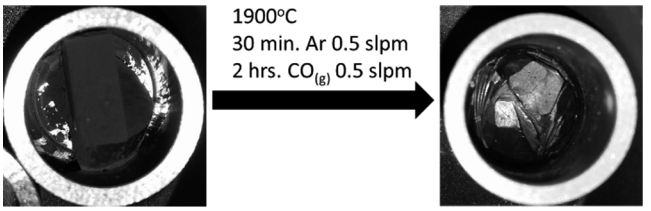

Figure 10. Initial experiment featuring reactants in $Nd_2O_2C_2$ stoichiometry, heated in an inert atmosphere before switching to CO(g) atmosphere.

moisture and quickly tarnished upon exposure to atmosphere, releasing extremely flammable acetylene gas.

According to the XRD analysis presented in Figure 11, the f11 sample was found to consist of $Nd_2O_2C_2$ and Nd_2O_3. These

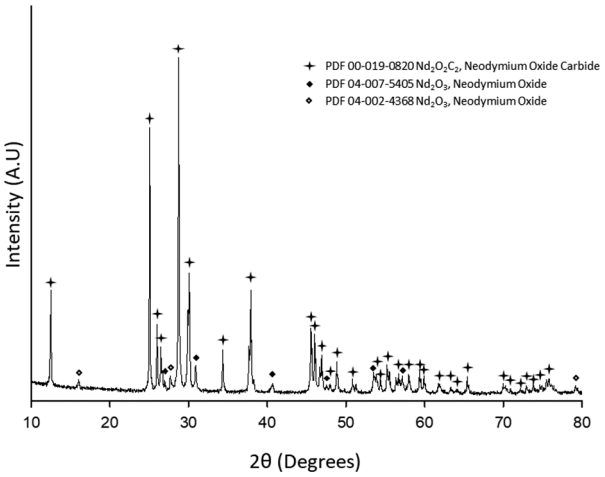

Figure 11. XRD analysis of a sample featuring $Nd_2O_2C_2$ stoichiometry subjected to initial heating in inert gas before changing to CO(g) at 1900 °C.

results lend further credibility to the assumption of release of CO(g) upon thermal decomposition, since a partial pressure of CO(g) exceeding that respective of the equilibrium decomposition reaction would be expected to reverse or inhibit thermal decomposition. The highest temperature (1900 °C) was chosen based on the results of the initial experiments, to ensure molten conditions, since such conditions were assumed to promote mass transfer.

Carbothermic Reduction in Graphite Resistance Furnace. A sample before and after reduction in a resistance heated graphite furnace at 1900 °C and atmosphere of continuously flushed inert gas are presented in Figure 12. f12

Upon examination of samples from the graphite resistance furnace, it was evident that the sample components had melted, forming a metallic appearing material that was reflective as can be seen in Figure 12. This material was found to adhere strongly to tungsten crucibles. Strong adhesion between crucible and sample material caused problems in sample extraction for analysis.

The best method of extraction was found to be milling of chips from the sample while submerged in mineral oil assumed to be inert to the components of the sample and crucible. Results from elemental mapping of a metal sample by EPMA are presented in Figure 13. A presence of two phases is evident, f13 one Nd rich phase (brighter) and one Cu rich phase (darker). Veins of the phase with low Nd concentration were observed

DOI: 10.1021/acs.iecr.8b03117
Ind. Eng. Chem. Res. XXXX, XXX, XXX−XXX

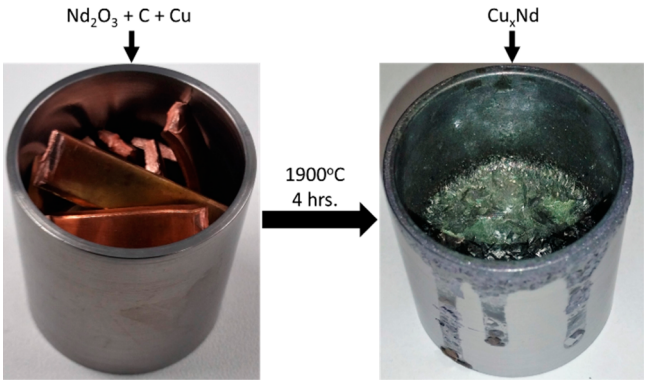

Figure 12. Image of a crucible containing reactant tablets and copper, before and after reduction in a graphite resistance furnace.

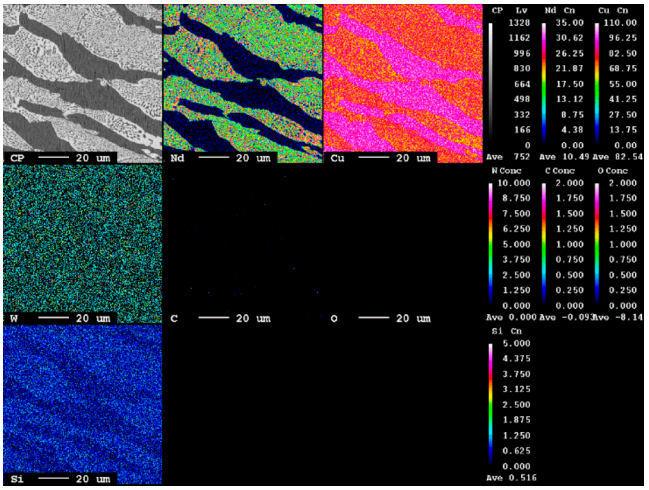

Figure 13. EPMA analysis of a sample from resistance heated graphite furnace featuring initial $Nd_2O_2C_2$ stoichiometry and final Cu_6Nd stoichiometry.

to be dispersed in the Nd rich phase as illustrated in Figure 13. The main elements present in the elemental map appear to be Nd, Cu, W, and Si. Carbon and oxygen were not detectable in the phase map at all. Tungsten seems to be randomly distributed in low concentration based on the color of the map and was included in the mapping to elucidate possible interactions between crucible and sample material. Small quantities of silicon appear to be distributed in the material with a slight preference toward a higher concentration in Nd rich phase; this element was included to evaluate possible contamination from silicon carbide (SiC) based abrasive discs utilized in sample preparation.

XRD analysis results of a sample having initial Nd oxide carbide stoichiometry and final Cu_6Nd stoichiometry are presented in Figure 14. The sample was found to consist of Cu_6Nd, $Nd_2O_2C_2$, Cu, and Nd_2O_3. Patterns of both Cu and Cu_6Nd were strong and easily identifiable whereas the peaks corresponding to neodymium oxide carbide and neodymium oxide were faint and thus more difficult to identify.

Quantified elemental composition by EPMA analysis of five different sample areas of the Nd rich phase in Figure 13 along with averaged values and corresponding standard deviations in Table 1. Main elemental constituents of this phase were found to be Nd, Cu, C, and O along with trace quantities of Si. Nd concentration in this phase is closely following that of $NdCu_6$,

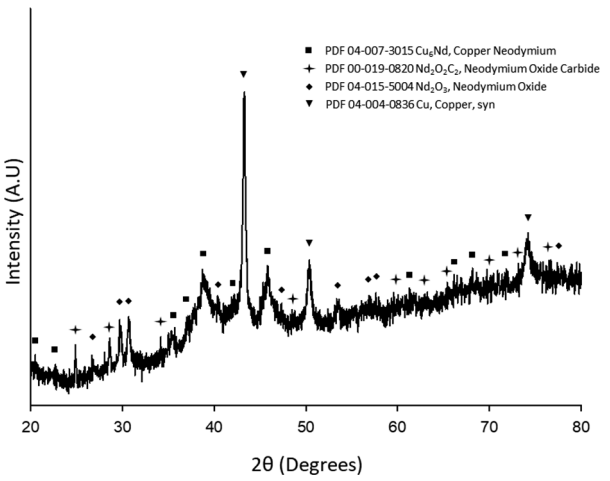

Figure 14. XRD results from a milled metal sample featuring initial $Nd_2O_2C_2$ stoichiometry and final Cu_6Nd stoichiometry.

Table 1. Average Elemental Composition of Five Areas in the Nd Rich Phase

element	O	W	C	Cu	Nd	Si
at % avg	1.11	0.00	0.40	85.02	13.41	0.07
std dev	0.15	0.00	0.27	0.33	0.15	0.08

which is also verified by XRD analysis presented in Figure 14. Elemental concentration of Si should however not be trusted since stated standard deviation is greater than reported element concentration. Quantified results do not conclusively support the existence of tungsten, despite observations in phase mapping and faint diffractions in XRD. Results with respect to tungsten are therefore not considered reliable.

Quantified results with respect to elemental distribution of five measured areas of the Cu rich phase in Figure 13 are presented in Table 2. Main elements appear to be Nd, Cu, C, and O. Despite results from the elemental map, tungsten and silicon were not found in this phase.

Table 2. Average Elemental Composition of Five Areas in the Cu Rich Phase

element	O	W	C	Cu	Nd	Si
at % avg	0.34	0.00	0.27	99.23	0.15	0.00
std dev	0.15	0.00	0.06	0.19	0.02	0.00

XRD results from experiments featuring initial $Nd_2O_2C_2$ stoichiometry with respect to Nd_2O_3/C ratio and final Cu_2Nd stoichiometry with respect to Cu/Nd ratio in graphite resistance furnace are illustrated in Figure 15. The copper quantity was chosen to coincide with $NdCu_2$ stoichiometry to evaluate how far the reaction would proceed with respect to achievable Cu−Nd intermetallics. Presence of Cu_5Nd, $Nd_2O_2C_2$, Nd_2O_3, NdC_2, and $WC_{0.5}$ are detected. XRD peaks corresponding to Cu_5Nd and Nd_2O_3 are strong and easily identifiable whereas patterns corresponding to $Nd_2O_2C_2$, NdC_2, and $WC_{0.5}$ are faint but identifiable.

Carbothermic Reduction in Arc Melter. Arc melted material was found to form a bead. To ensure homogeneity and completion of the reaction, this bead was turned over and remelted repeatedly. A visual example on the arc melting

DOI: 10.1021/acs.iecr.8b03117
Ind. Eng. Chem. Res. XXXX, XXX, XXX−XXX

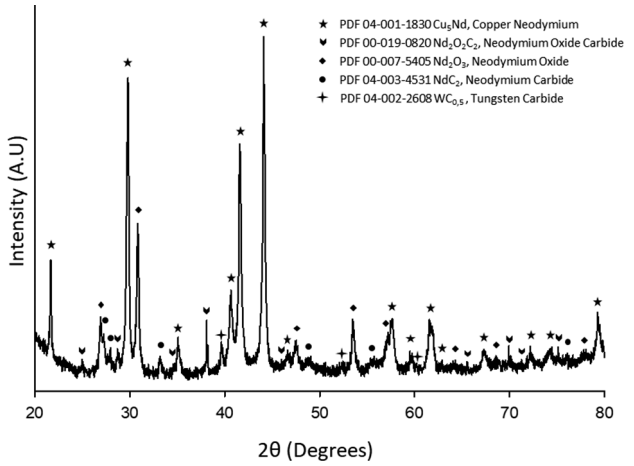

Figure 15. XRD results for experiments featuring initial $Nd_2O_2C_2$ stoichiometry and final Cu_2Nd stoichiometry in a graphite furnace.

f16 507 process from initial reactants to final product is presented in
f16 508 Figure 16.

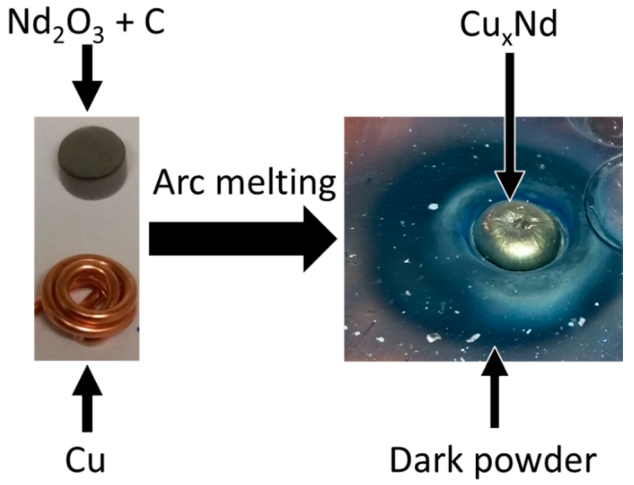

Figure 16. Arc melting process, from initial reactants to final product.

509 After the final arc melting sequence, a fine dark powder with
510 small flakes of bright colored material was found to surround
511 the bead of melted material. An XRD analysis of this powder is
512 presented in Figure 20.
513 Results from EPMA analysis of material subjected to arc
f17 514 melting can be observed in Figure 17. This material featured an
515 initial $Nd_2O_2C_2$ stoichiometry with respect to Nd_2O_3/C ratio
516 and a final stoichiometry of Cu_2Nd with respect to Cu/Nd
517 ratio. Again, EPMA phase mapping revealed two phases, one
518 containing higher concentration of Nd (brighter) whereas the
519 other contains more Cu (darker). Samples from arc melting
520 displayed irregular areas that based on contents and
521 concentration of respective elements likely were representative
522 of unconverted material. This unconverted material seemed to
523 have a predominance for areas enriched in Nd. Elemental
524 constituents were found to be Nd, Cu, W, C, O, and Si. Silicon
525 appears slightly more frequent in the Nd rich phase and was
526 included in the analysis to evaluate if silicon carbide (SiC)
527 particulate matter from the abrasive discs used in preparation
528 of the samples could be embedded in the soft sample material.
529 Tungsten does indeed again appear on the phase map,

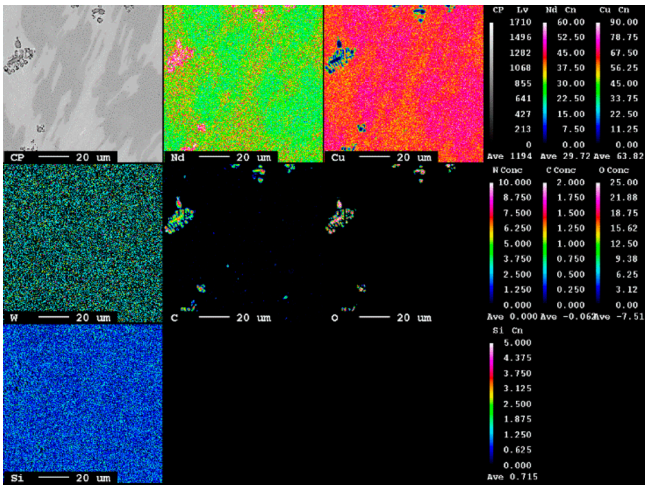

Figure 17. EPMA mapping of the elemental distributions in a sample from an arc melting experiment featuring initial $Nd_2O_2C_2$ stoichiometry and final Cu_2Nd stoichiometry.

randomly distributed in the material just as it did for samples 530
prepared by graphite resistance furnace. This result is 531
surprising since the experiment was devised to minimize 532
probability of tungsten contamination by exchanging the arc 533
furnace electrode which normally consists of tungsten with one 534
made from graphite. The only possible route of contamination 535
would thus be the initial ring milling of the reactants that was 536
identical for all experimental runs. Quantified results do 537
however not show any detectable concentration of W and the 538
results from phase mapping should thus not be considered 539
reliable. Nevertheless, a presence of tungsten could possibly 540
indicate a similar reaction as suggested by Mcallum et al., 541
where carbon from decomposed NdC_2 is captured by 542
formation of very stable tungsten carbide which is expected 543
to be finely distributed in the final reaction products.[16] Upon 544
investigation of this assumption, one can address the quantified 545
results of Table 3 and Table 4 as well as XRD results presented 546 t3t4f18

Table 3. Averaged Elemental Composition of Five Measured Areas in the Nd Rich Phase from Arc Melting

element	O	W	C	Cu	Nd	Si
at % avg	1.57	0.01	0.20	79.13	18.93	0.15
std dev	0.18	0.02	0.02	0.42	0.35	0.02

Table 4. Averaged Elemental Composition of Five Measured Areas in the Cu Rich Phase from Arc Melting

element	O	W	C	Cu	Nd	Si
at % avg	1.13	0.00	0.24	84.53	14.02	0.09
std dev	0.08	0.00	0.01	0.05	0.11	0.06

in Figure 18, which by the lack of W detection in conjunction 547 f18
with low concentration of carbon would suggest that such a 548
scenario to be unlikely, since a significant quantity of tungsten 549
would have to be present to consume all carbon from the 550
formed carbide to release elemental Nd. 551

The XRD analysis of an arc melted sample featuring initial 552
$Nd_2O_2C_2$ stoichiometry and final Cu_2Nd stoichiometry is 553
presented in Figure 18. The sample was found to consist of 554
Cu_5Nd, Cu_6Nd, Nd_2O_3, and $Nd_2O_2C_2$. It should be mentioned 555
that these samples featured a reactivity that necessitated short 556

DOI: 10.1021/acs.iecr.8b03117
Ind. Eng. Chem. Res. XXXX, XXX, XXX−XXX

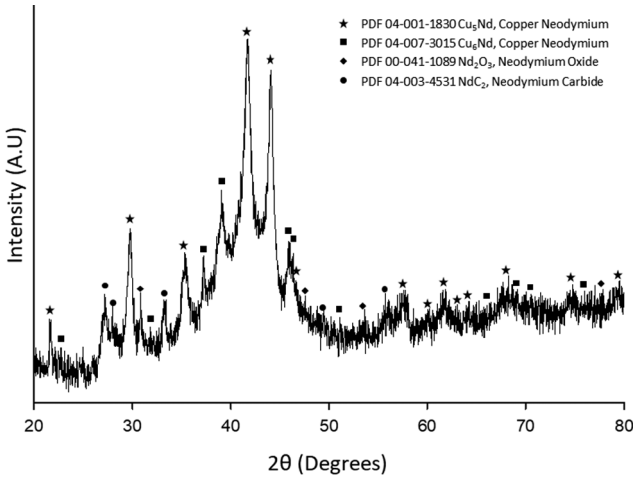

Figure 18. XRD analysis results from an arc melted sample featuring reduced initial stoichiometry of $Nd_2O_2C_2$ and final stoichiometry of Cu_2Nd.

analysis times to avoid detrimental interaction with atmospheric species. These results are corroborated by the quantified results of Table 3, suggesting the phase enriched in Cu to be closely corresponding with that of Cu_6Nd along with Table 4, which describes the Nd enriched phase to consist of material corresponding to that of Cu_5Nd.

Quantified elemental composition of five areas representative of the Nd-rich phase in Figure 17 is given in Table 3. In this phase, traces of W could be detected along with small quantities of silicon. Results with respect to tungsten were considered unreliable since the standard deviation was found to exceed that of the reported element concentration.

Quantified elemental composition corresponding to the Cu-rich phase of Figure 17 is presented in Table 4. Tungsten does not appear to be present in any of the analyzed areas. Silicon appears to exist in slightly lower quantities than in phases from the same sample featuring elevated concentrations of Nd.

Results from XRD analysis of a sample featuring an increase in carbon quantity of 18% weight in excess of $Nd_2O_2C_2$ stoichiometry, and Cu/Nd ratio of Cu_6Nd are presented in Figure 19. This was done to evaluate effect of excess carbon upon experimental results. The sample was found to consist of Cu_6Nd, Nd_2O_3, NdC_2, and Cu. Patterns corresponding to Cu_6Nd and Cu were found to be clear and easy to identify, whereas patterns respective of Nd_2O_3 and NdC_2 was faint but identifiable.

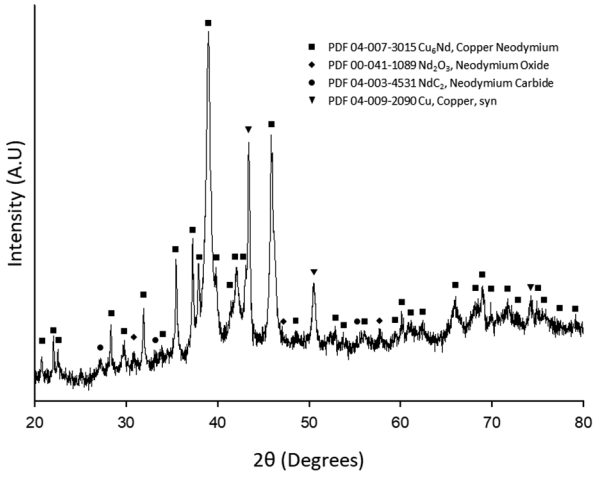

Figure 19. XRD results from experiments featuring use of arc melter and 18% weight excess carbon as compared to $Nd_2O_2C_2$ stoichiometry and Cu/Nd ratio of final $NdCu_6$ stoichiometry.

The dark powder featuring bright chunks of material in Figure 16 was found to consist of fine copper particles, neodymium oxide, and neodymium oxide carbide, as shown by the XRD analysis presented in Figure 20. Copper was likely evaporated by the intense heat of arc melting whereas Nd_2O_3 and $Nd_2O_2C_2$ were likely rejected from molten material upon solidification.

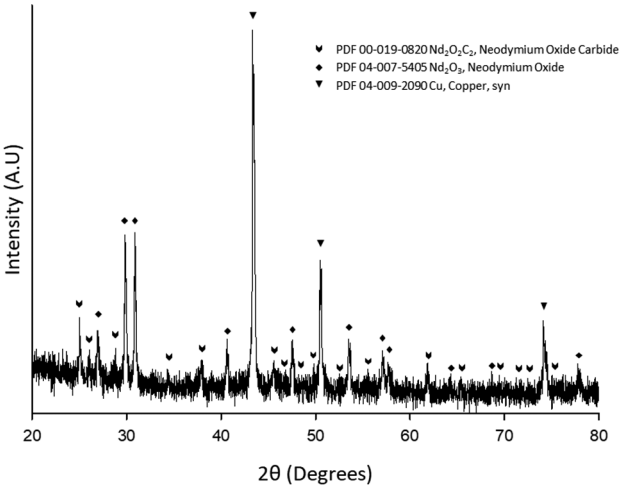

Figure 20. XRD analysis of dark powder assumed to be evaporated from sample during arc melting.

DISCUSSION

Decomposition and Melting Behavior of the $Nd_2O_2C_2$ Compound. A set of initial experiments were performed to evaluate melting behavior of the neodymium oxide carbide phase. This phase was chosen since it was thought to have a favorable carbon−oxygen balance, allowing for the formation and continuous flushing of gaseous reaction products (CO(g)) during reduction with metal solvent. According to analysis of reaction products as presented in Figure 4 and Figure 5, the mixture had been partially molten and found to consist of $Nd_2O_2C_2$ and Nd_2O_3. The melting phenomena is also described by Butherus et al., who claimed that the $Nd_2O_2C_2$ compound started to melt partially at 1592 °C and completely at 1602 °C, agreeing well with the experimental observations of this work.[26] Thus, to ensure molten conditions in shorter time, the temperature was increased. Based on the results of this experiment as presented in Figure 6 and Figure 7, it was inferred that thermal decomposition of the $Nd_2O_2C_2$ phase was occurring at this temperature. The effect of partial pressure of CO(g) on the previously observed thermal decomposition reaction are presented in Figures 8−11. Based on these results, it was assumed that carbon monoxide in excess of equilibrium pressure forced the equilibrium reaction toward the reactant side, inhibiting decomposition of $Nd_2O_2C_2$. Therefore, it would also likely mean that thermal decomposition of $Nd_2O_2C_2$ is associated with evolution of CO(g). Thus, a plausible total reaction equation describing the thermal decomposition reaction of $Nd_2O_2C_2$ could be represented by

DOI: 10.1021/acs.iecr.8b03117
Ind. Eng. Chem. Res. XXXX, XXX, XXX−XXX

reaction 3, which was also proposed by Butherus et al.[26] The fact that the reaction mixture had fused during thermal decomposition could indicate existence of a eutectic mixture of Nd_2O_3 and NdC_2. The possibility of a eutectic based upon observations of fused samples upon extraction is also mentioned by Butherus et al.[26] In that work it was concluded that the eutectic was a result of reaction between $Nd_2O_2C_2$ and the graphite crucible.[26] In this work, tungsten crucibles were utilized, hence limiting available carbon. Since the samples were still observed to be fused by use of tungsten crucibles it would be prudent to assume that any eutectic formed would thus be a consequence of the mixture of Nd_2O_3 and NdC_2 and not reaction between $Nd_2O_2C_2$ and graphite. Use of the $Nd_2O_2C_2$ stoichiometry at a temperature of 1900 °C encountered in these experiments would thus indicate that all components were molten which would promote mass transfer, ultimately reducing time for carbothermic reduction of Nd_2O_3 and subsequent formation of Cu−Nd intermetallics.

Cu−Nd Intermetallic Formation Mechanism. To evaluate possible effects on final product distribution and to possibly get information on reaction mechanisms responsible for the observed reactions, reactants were mixed in various stoichiometric ratios and reduced (Table S2, Supporting Information). As can be seen from results of both graphite resistance furnace and arc melter experiments, Nd_2O_3 was found in varying concentrations in all samples. Diffraction patterns corresponding to this compound was found to drop as carbon quantity was increased. This is evident upon comparison of Figure 14 and Figure 19. Such a result is unsurprising upon consideration of the decomposition reaction 3 and one would assume excess carbon equating to formation of more NdC_2 by reduction of Nd_2O_3. An increase of intensity with respect to NdC_2 XRD patterns could thus be expected. According to results, this was not found to be the case, NdC_2 was virtually nonexistent in samples featuring stoichiometric quantities of carbon and only faint reflections respective of NdC_2 and Nd_2O_3 could be detected in samples featuring higher carbon concentration.

When considering results with respect to Cu−Nd intermetallics, increased carbon concentration along with maintaining quantities of copper indicative of a certain Cu−Nd stoichiometry yielded stronger diffraction patterns for products corresponding to the desired Cu−Nd intermetallic, indicative of increased concentration and crystallinity of the compound. As an example of the previous statement, by comparison of Figure 14 and Figure 19, one can see that using a C−Cu−Nd_2O_3 stoichiometry corresponding to that of $Nd_2O_2C_2$ and Cu_6Nd yielded a mixture of Nd_2O_3, Cu_6Nd (faint diffraction pattern), and unconverted Cu (strong diffraction pattern), whereas experiments featuring otherwise identical composition, save for higher carbon concentration, resulted in formation of Cu_6Nd with a much higher intensity diffraction pattern. These results combined with the observation of only faint diffractions corresponding to NdC_2 are thus pointing in the direction of the reaction mechanism being decomposition of NdC_2. This decomposition is likely promoted by presence of molten copper, reducing activity of solvated Nd species to a value below that required by the equilibrium constant to sustain NdC_2 at the given temperature. The reduction in activity for Nd species solvated by copper means that the Cu−Nd mixture has a negative deviation from ideality and is an indication of strong interaction occurring between the Cu and Nd species in the molten mixture.[21] Decomposition of neodymium dicarbide has previously been described in literature and was found to result in formation of elemental Nd and carbon.[34,35] According to the literature, decomposition of NdC_2 has occurred under vacuum conditions, which differs from the atmospheric pressure inert gas used in the current experiments. The proposed reaction mechanism based on carbothermic reduction of Nd_2O_3 and subsequent decomposition of both $Nd_2O_2C_2$ and NdC_2, forming Cu−Nd intermetallics, is illustrated in Scheme 1.

Scheme 1. Reaction Mechanism of Carbothermic Nd_2O_3 Reduction and Subsequent Cu−Nd Formation

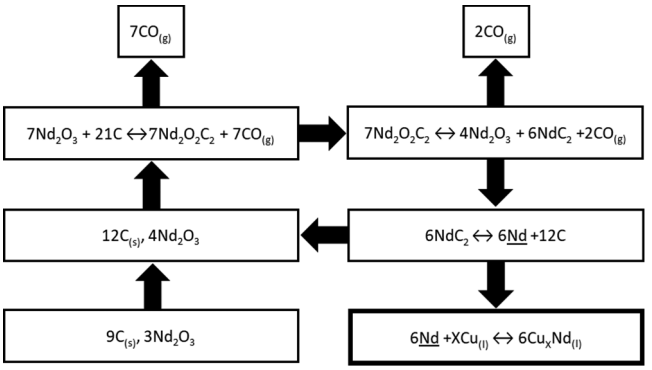

It should be noted that NdC_2 and $Nd_2O_2C_2$ are very sensitive to atmospheric moisture, rapidly decomposing, forming acetylene gas and Nd_2O_3.[26] Sample extraction by milling for EPMA analysis and subsequent fine grinding of sample material for XRD analysis could provide possible pathways to exposure with regards to atmospheric moisture, even when samples were coated in oil. In this regard, the probability of atmospheric moisture interfering with analysis results becomes higher for samples subjected to XRD analysis due to an extra grinding step. Thus, the possibility of phases appearing and/or disappearing in XRD that might exist in the original sample material should not be disregarded although careful sample preparation was aimed at mitigating these risks.

Extent of Cu−Nd Intermetallic Formation. Reactant ratio with respect to Cu and Nd_2O_3 was varied from Cu_6Nd to Cu_2Nd stoichiometry. This was done to evaluate how far the reduction reaction would proceed with respect to maximum attainable Cu−Nd intermetallic and is hereafter referred to as extent of intermetallic formation. According to available literature, several intermetallics exists in the Cu−Nd system (see reaction eqs 6a−f).[23,30,31] If decomposition of NdC_2, caused by a reduction in activity of Nd species is responsible for the formation of Cu−Nd intermetallics as assumed previously, it would also be prudent to assume that at some concentration of Nd in Cu, the activity of Nd would approach the value required to reform NdC_2. At such conditions, an equilibrium would be expected to occur between NdC_2 and the Cu−Nd intermetallic with the highest attainable Nd concentration. The maximum attainable Cu−Nd intermetallic could thus be gauged by simultaneous presence of NdC_2 and the specific Cu−Nd intermetallic featuring the highest concentration of Nd, found to exist at these conditions. According to results presented in Figure 15, experiments featuring Cu_2Nd stoichiometry, appeared to stop at Cu_5Nd, leaving a mixture of Cu_5Nd and NdC_2 along with $Nd_2O_2C_2$ and Nd_2O_3. For experiments performed by arc melting of an

DOI: 10.1021/acs.iecr.8b03117
Ind. Eng. Chem. Res. XXXX, XXX, XXX−XXX

identical reactant mixture, reaction products were found to be Cu_6Nd, Cu_5Nd, NdC_2 and Nd_2O_3 as presented in Figure 18. These results are thus indicative of the maximum attainable concentration of Nd in Cu corresponding to that of Cu_5Nd, never reaching that of Cu_2Nd although enough Nd exists in the system to theoretically facilitate this phase. When activity of solvated Nd exceeds that required in formation of intermetallics, compounds such as Cu_6Nd and Cu_5Nd is formed upon cooling. Formation of such intermetallics has a negative Gibbs energy and is spontaneous, likely affecting the net energy of the reduction reaction. Another interesting result is the coexistence of $Nd_2O_2C_2$ and Cu−Nd intermetallics, since presence of $Nd_2O_2C_2$ necessitates a certain partial pressure of CO(g) to avoid decomposition at temperatures encountered during experiments. This likely means that the Cu−Nd intermetallics have low sensitivity to partial pressure of CO(g) with respect to potential decomposition of the intermetallic, yet again pointing in direction of Nd having low activity in Cu. Partial pressure of CO(g) is still important since it facilitates decomposition of $Nd_2O_2C_2$ giving rise to a liquid mixture of Nd_2O_3 and NdC_2 which in turn was thought to enhance reaction rate by increased mass transfer.

Potential for Industrial Production of Pure Nd from Cu−Nd Intermetallics. Separation of Cu−Nd products from other components of the reaction was not attempted, nor was any attempt made to quantify level of conversion. With respect to possible future product separation one might compare Figure 13 and Figure 17. It seems that experiments performed in graphite furnace are less contaminated with inclusions of unconverted material after experiments than experiments utilizing arc melter. This might be caused by slightly different mixing and slower cooling in the graphite furnace. These observations can indicate that a separation occurs between the metallic phase and other reaction products. Observed evaporation of copper during arc melting (evident from XRD results of dark powder as presented in Figure 20) is interesting since it opens for facile concentration of elemental neodymium from carbothermic reduction and warrants further investigation. This evaporative method of Nd "up-concentration" would require carbon to be unavailable in the system since it could cause a potential back reaction reforming the dicarbide, thus necessitating an optimization with respect to carbon quantities utilized in the reduction. The ease of reduction as demonstrated by arc melting experiments suggest a potential for future scalation of the process by utilizing an industrial electric arc furnace. Ongoing research on Nd electrowinning has demonstrated potential of allowing for extraction of pure Nd from Cu−Nd intermetallics.[36]

CONCLUSIONS

The path and mechanism of carbothermic reduction of neodymium(III) oxide in the presence of molten copper, to form neodymium−copper intermetallics, were studied through arc melting as well as graphite resistance furnace experiments. The following conclusions were reached:

1. Carbothermic reduction of neodymium(III) oxide was found to be feasible by utilizing copper as a solvent metal in both resistance heated graphite furnace and by arc melting, resulting in formation of Cu−Nd intermetallic phases, predominantly Cu_6Nd and Cu_5Nd. The reaction did not seem to go past Cu_5Nd, in terms of Nd concentration, as an intermetallic product.
2. The proposed reaction mechanism was decomposition of neodymium carbide, which is a product of thermal decomposition of neodymium oxide carbide formed in the reaction of neodymium(III) oxide with carbon.
3. Use of excess quantity of carbon as compared to Nd oxide carbide stoichiometry in the initial raw material mixture was found to correlate with increased yield of the desired Cu−Nd intermetallic.
4. Removal of CO(g) was important with respect to the extent of Cu−Nd intermetallic formation, since it facilitated increased decomposition of $Nd_2O_2C_2$, forming a molten mixture consisting of Nd_2O_3 and NdC_2 along with evolution of CO(g).
5. While important that CO is removed to facilitate $Nd_2O_2C_2$ decomposition, the process was found to be relatively insensitive to partial pressure of carbon monoxide as evident from coexistence of both Cu−Nd intermetallic along with $Nd_2O_2C_2$

ASSOCIATED CONTENT

Supporting Information

The Supporting Information is available free of charge on the ACS Publications website at DOI: 10.1021/acs.iecr.8b03117.

Table S1 (initial experimental parameters) and Table S2 (main experimental parameters) (PDF)

AUTHOR INFORMATION

Corresponding Author

*E-mail: ivar.a.odegard@ntnu.no.

ORCID

Ivar A. Ødegård: 0000-0003-1279-4744

Notes

The authors declare no competing financial interest.

ACKNOWLEDGMENTS

The work was funded through the framework of the E.U financed REECOVER project under Contract No. 62311205. Funding of the Ph.D. position of the first author by the Norwegian University of Science and Technology is gratefully acknowledged.

ABBREVIATIONS

REE = rare earth elements
EPMA = electron microprobe analyzer
XRD = X-ray diffraction
slpm = standard liter per minute
e.g. = example given
A.U. = arbitrary unit

REFERENCES

(1) Binnemans, K.; Jones, P. T.; Blanpain, B.; Van Gerven, T.; Yang, Y.; Walton, A.; Buchert, M. Recycling of rare earths: a critical review. *J. Cleaner Prod.* **2013**, *51*, 1−22.

(2) Guyonnet, D.; Planchon, M.; Rollat, A.; Escalon, V.; Tuduri, J.; Charles, N.; Vaxelaire, S.; Dubois, D.; Fargier, H. Material flow analysis applied to rare earth elements in Europe. *J. Cleaner Prod.* **2015**, *107*, 215−228.

(3) Massari, S.; Ruberti, M. Rare earth elements as critical raw materials: Focus on international markets and future strategies. *Resour. Policy* **2013**, *38* (1), 36−43.

DOI: 10.1021/acs.iecr.8b03117
Ind. Eng. Chem. Res. XXXX, XXX, XXX−XXX

(4) McLellan, B. C.; Corder, G. D.; Golev, A.; Ali, S. H. Sustainability of the Rare Earths Industry. *Procedia Environ. Sci.* **2014**, *20*, 280−287.
(5) Krishnamurthy, N.; Gupta, C.K. *Extractive Metallurgy of Rare Earths*; CRC Press, 2004.
(6) Lucas, J., Lucas, P.; Le Mercier, T.; Rollat, A.; Davenport, W. Chapter 6: Production of Rare Earth Metals and Alloys—Electrowinning. In *Rare Earths*; Elsevier: Amsterdam, The Netherlands, 2015; pp 93−108.
(7) Singh, S.; Juneja, J. M.; Bose, D. K. Preparation of neodymium-iron alloys by electrolysis in a fused chloride bath. *J. Appl. Electrochem.* **1995**, *25* (12), 1139−1142.
(8) Kaneko, A.; Yamamoto, Y.; Okada, C. Proceedings of the International Conference, Rare Earths '92 Electrochemistry of rare earth fluoride molten salts. *J. Alloys Compd.* **1993**, *193* (1), 44−46.
(9) Gupta, C. K.; Krishnamurthy, N. The Rare Earths. In *Extractive Metallurgy of Rare Earths*; CRC Press, 2004.
(10) Anderson, R. N.; Parlee, N. A. D. *Carbothermic Reduction Method for Converting Metal Oxides to Metal Form*; Parlee Anderson Corporation, 1974.
(11) Anderson, R. N.; Parlee, N. A. D. Carbothermic reduction of refractory metals. *J. Vac. Sci. Technol.* **1976**, *13* (1), 526−529.
(12) Eckert, C. A.; Irwin, R. B.; Graves, C. W. Liquid metal solvent selection: the magnesium oxide reduction reaction. *Ind. Eng. Chem. Process Des. Dev.* **1984**, *23* (2), 210−217.
(13) Gschneidner, J. K. A.; Schmidt, F. A. *Method for Producing La/Ce/MM/Y Base Alloys, Resulting Alloys, and Battery Electrodes*. U.S. Patent 9,525,176, December 20, 2016.
(14) Gschneidner, K. A., Schmidt, F. A.; McCallum, R. W.; Iowa State University Research Foundation, Inc. *Method for Producing Permanent Magnet Materials and Resulting Materials*. World Patent WO2011053352, May 5, 2011.
(15) Howell, W. J.; Eckert, C. A.; Anderson, R. N. Carbothermic Reduction Using Liquid Metal Solvents. *JOM* **1988**, *40* (7), 21−23.
(16) McCallum, R. W., Ellis, T. W.; Dennis, K. W.; Hofer, R. J.; Branagan, D. J.; Iowa State University Research Foundation, Inc. *Production Method for Making Rare Earth Compound*, U.S. Patent 5,690,889, November 15, 1997.
(17) Selvaduray, G. S. The Liquid Tin Process: An Experimental Investigation of a Potential Pyrometallurgical Process for Reprocessing Irradiated Carbide Fuel From Fast Breeder Reactors. *Eur. Appl. Res. Rep., Nucl. Sci. Technol. Sect.* **1983**, *4* (6), 1451−1514.
(18) Staggers, J. O.; Foote Mineral Company *Rare Earth Metal Silicide Alloys*. U.S. Patent 4,018,597, April 19, 1977.
(19) Gupta, C. K.; Krishnamurthy, N. Reduction. In *Extractive Metallurgy of Rare Earths*; CRC Press, 2004.
(20) Heckman, R. A. *Molten tin reprocessing of spent nuclear fuel elements*. U.S. Patent 4,392,995, July 12, 1983.
(21) Guisard Restivo, T. A.; Capocchi, J. D. T. Carbothermic reduction of uranium oxides into solvent metallic baths. *J. Nucl. Mater.* **2004**, *334* (2−3), 189−194.
(22) Li, X.; Colombo, L.; Ruoff, R. S. Synthesis of Graphene Films on Copper Foils by Chemical Vapor Deposition. *Adv. Mater.* **2016**, *28* (29), 6247−6252.
(23) Wang, P.; Zhou, L.; Du, Y.; Xu, H.; Liu, S.; Chen, L.; Ouyang, Y. Thermodynamic optimization of the Cu−Nd system. *J. Alloys Compd.* **2011**, *509* (6), 2679−2683.
(24) Laks, C.; Pelleg, J.; Zevin, L. Notes on the Nd-Cu system. *J. Less-Common Met.* **1984**, *102* (1), 23−28.
(25) Carnasciali, M. M.; Costa, G. A.; Franceschi, E. A. Phase equilibria in the Nd-Cu system. *J. Less-Common Met.* **1983**, *92* (1), 97−103.
(26) Butherus, A. D.; Leonard, R. B.; Buchel, G. L.; Eick, H. A. The Preparation and Some Properties of Nd2O2C2. *Inorg. Chem.* **1966**, *5* (9), 1567−1571.
(27) Vidhya, R.; Antony, M. P.; Vasudeva Rao, P. R.; Viswanathan, B. Enthalpy and Gibbs energy of formation of neodymium dicarbide. *J. Nucl. Mater.* **2001**, *295* (2−3), 228−232.
(28) Butherus, A. D. *Lanthanide Oxycarbides: Phase and Equilibrium Studies*. Ph.D. Thesis, Michigan State University, East Lansing, MI, 1969.
(29) Anti Roine, P. L.; Mansikka-aho, J.; Björklund, P.; Kentala, J.-P.; Talonen, T.; Kotiranta, T.; Ahlberg, R.; Gröhn, A.; Saarinen, O.; Myyri, J.; Sipilä, J.; Vartainen, A. *HSC Chemistry 7*; Outotec Research Center, 2011.
(30) Subramanian, P. R.; Laughlin, D. E. The Cu–Nd(Copper–Neodymium) System. *Bull. Alloy Phase Diagrams* **1988**, *9*, 362.
(31) Predel, B., Cu-Nd (Copper-Neodymium). In *Cr−Cs−Cu−Zr*; Madelung, O., Ed.; Springer Berlin Heidelberg: Berlin, Heidelberg, Germany, 1994; pp 1−3.
(32) Zhuang, W.; Qiao, Z.-Y.; Wei, S.; Shen, J. Thermodynamic evaluation of the Cu-R (R: Ce, Pr, Nd, Sm) binary systems. *J. Phase Equilib.* **1996**, *17* (6), 508−521.
(33) Bale, C. W.; Bélisle, E.; Chartrand, P.; Decterov, S. A.; Eriksson, G.; Gheribi, A. E.; Hack, K.; Jung, I. H.; Kang, Y. B.; Melançon, J.; Pelton, A. D.; Petersen, S.; Robelin, C.; Sangster, J.; Spencer, P.; Van Ende, M. A. FactSage thermochemical software and databases, 2010−2016. *CALPHAD: Comput. Coupling Phase Diagrams Thermochem.* **2016**, *54*, 35−53.
(34) Downing, J. H.; Gorski, H. L.; Koerner, E. L., Jr. *Production of Rare Earth Metals*; Union Carbide Corp.: Houston, TX, 1963.
(35) Faircloth, R. L.; Flowers, R. H.; Pummery, F. C. W. Vaporization of some rare-earth dicarbides. *J. Inorg. Nucl. Chem.* **1968**, *30* (2), 499−518.
(36) Sun, C.; Xiao, Y.; Xu, Q.; Yang, Y. The Separation of Nd from Cu6Nd Alloy by Electrolysis. In *Technical University Delft Department of Materials Science and Engineering Technology Day*, Delft, The Netherlands, June 2018; poster presentation.

DOI: 10.1021/acs.iecr.8b03117
Ind. Eng. Chem. Res. XXXX, XXX, XXX−XXX